2013

A mathematical function to represent S-shaped relationships for geotechnical applications

Martin D. Liu
University of Wollongong, martindl@uow.edu.au

K J. Xu
Pb Americas, Incorporated

Suksun Horpibulsuk
Suranaree University of Technology, suksun@g.sut.ac.th

Publication Details

Liu, M. D., Xu, K. J. & Horpibulsuk, S. (2013). A mathematical function to represent S-shaped relationships for geotechnical applications. Institution of Civil Engineers. Proceedings. Geotechnical Engineering, 166 (GE3), 321-327.

A mathematical function to represent S-shaped relationships for geotechnical applications

Abstract
In this paper a new mathematical function is proposed for describing the S-shape relationship in both normal x and y scale and the semi-logarithmic x and y scale. Basic features of the proposed function have been demonstrated. The proposed function has then been used to simulate the S-shape relationship for seven categories of engineering phenomena. It is seen that the proposed mathematical function has a great potential for representing various S-shape relationships and provides a powerful tool for characterising properties of materials or response of systems; it is thus useful for further numerical analysis.

Keywords
relationships, shaped, represent, applications, function, geotechnical, mathematical

Disciplines
Engineering | Science and Technology Studies

Publication Details
Liu, M. D., Xu, K. J. & Horpibulsuk, S. (2013). A mathematical function to represent S-shaped relationships for geotechnical applications. Institution of Civil Engineers. Proceedings. Geotechnical Engineering, 166 (GE3), 321-327.

Geotechnical Engineering
Volume 166 Issue GE3

A mathematical function to represent S-shaped relationships for geotechnical applications
Liu, Xu and Horpibulsuk

ice | proceedings

Proceedings of the Institution of Civil Engineers
Geotechnical Engineering 166 June 2013 Issue GE3
Pages 321–327 http://dx.doi.org/10.1680/geng.10.00029
Paper 1000029
Received 11/03/2010 Accepted 02/02/2011
Published online 03/06/2012
Keywords: geotechnical engineering/mathematical modelling/strength & testing of materials

ice Institution of Civil Engineers publishing

A mathematical function to represent S-shaped relationships for geotechnical applications

1 **Martin D. Liu** MPhl, PhD
Senior Lecturer, University of Wollongong, New South Wales, Australia

2 **K. J. Xu** PhD
PB Americas, Incorporated, New York, USA

3 **Suksun Horpibulsuk** MEng, PhD
Professor, Suranaree University of Technology, Nakhon Ratchasima, Thailand



In this paper a new mathematical function is proposed for describing the S-shape relationship in both normal *x* and *y* scale and the semi-logarithmic *x* and *y* scale. Basic features of the proposed function have been demonstrated. The proposed function has then been used to simulate the S-shape relationship for seven categories of engineering phenomena. It is seen that the proposed mathematical function has a great potential for representing various S-shape relationships and provides a powerful tool for characterising properties of materials or response of systems; it is thus useful for further numerical analysis.

1. Introduction

In engineering practice and in physics it has been frequently observed that a characteristic of a material or a response of a system, that is an assembly of a number of objects with finite or infinite sizes, to an external agent may form an S-shaped curve either in normal coordinates or in semi-logarithmic coordinates. For example, the variation of soil strength with the clay fraction has an S-shape relationship in normal coordinates (Figure 1(a), from Lupini *et al.* (1981)). In the figure, φ_{cs} and φ_r represent the critical state friction angle and the residual friction angle, respectively, and ω_c represents the clay fraction. The compression curves for geomaterials under first loading are S-shaped in the semi-logarithmic scale (Figure 1(b), from Pestana and Whittle (1995)). In the figure e represents the voids ratio, and σ'_v represents the vertical effective stress. The consolidation deflection of a raft on a deep layer of soil plotted against time is an S-shape relationship (Figure 1(c), from Booker and Small (1984)).

A mathematical description of the characteristics of materials is useful for numerical interpretation of material properties. However, more importantly, a functional expression for the material property is essential for further numerical analysis. The present authors are not aware of such mathematical formulae that give a reliable description of the whole S-shape relationship. Taking the compression behaviour of soil as an example, the compression equation forms a base for most constitutive modelling of soils and some important geotechnical computations (Burland, 1990; Horpibulsuk *et al.*, 2010; Liu and Carter, 2003; Pestana and Whittle, 1995; Suebsuk *et al.*, 2010, 2011). Because there is no efficient way to describe the whole S-shape compression relationship, a common way to describe it is to divide the curve into several segments and then the segment or the segments of interest are modelled by linear relationships (Butterfield and Baligh, 1996; Khalili *et al.*, 2005; Terzaghi and Peck, 1948). In the current paper, a new single mathematical function is proposed for describing the S-shape relationship. The capacities of the S-shape function are demonstrated and evaluated by simulating various S-shape events.

2. Proposed mathematical function for the S-shape relationship

2.1 Proposed equation

The proposed mathematical function for S-shape relationships is expressed as follows

$$y = \pm \frac{a_1}{x}\left[1 + (x-1)e^{-a_2 x^{a_3}}\right] + b \quad (1)$$

The first part of the function may take a positive sign in order to simulate the S-shape relationship where y decreases monotonically, and may take a negative sign to simulate the S-shape

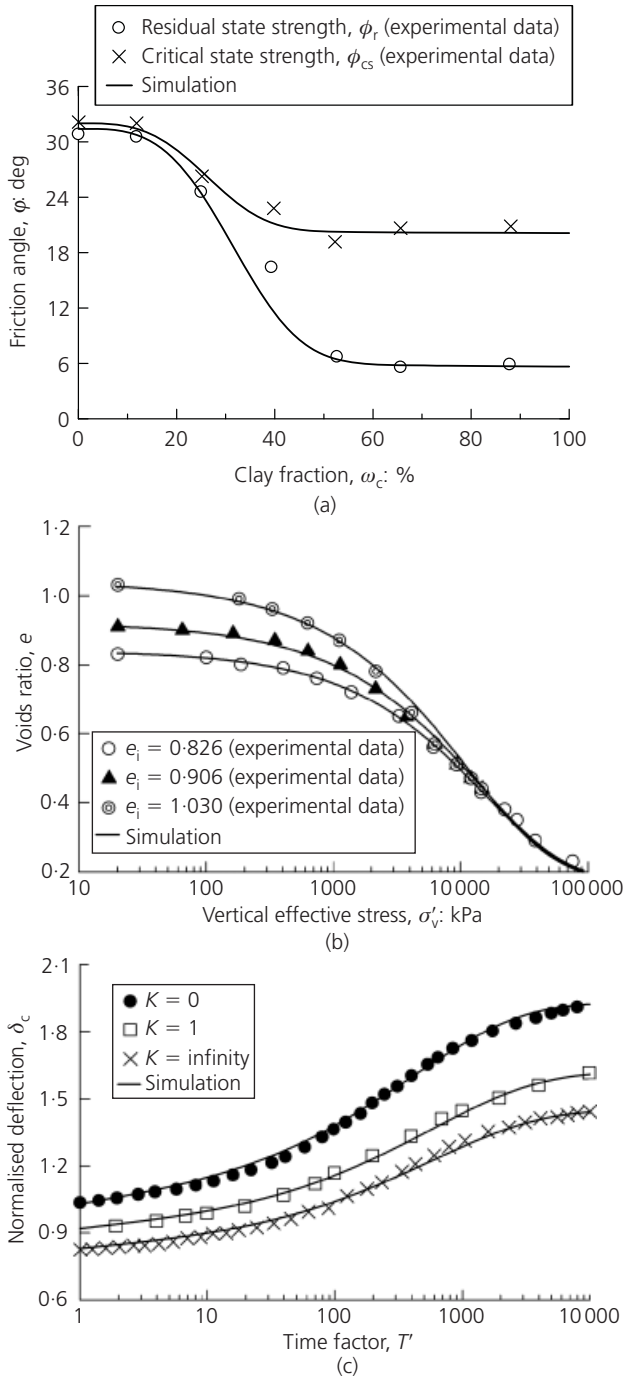

Figure 1. (a) Variation of the strength of soil with clay fraction (data after Lupini *et al.* (1981)). (b) One-dimensional compression behaviour of Quiou sand (data after Pestana and Whittle (1995)). (c) Time–deflection of circular raft with flexibility K (theoretical data after Booker and Small (1984))

relationship where y increases monotonically. There are four parameters in the new function: a_1, a_2, a_3 and b. Parameters a_1, a_2, a_3 are assumed to be positive. Mathematically, the valid range for variable x, which is dependent on a_3, is given as follows

$$2. \quad \begin{cases} x \geqslant 0 & \text{for } a_3 \geqslant 1 \\ x > 0 & \text{for } 0 < a_3 < 1 \end{cases}$$

However, for a practical application, the physical meaning of the variable may impose its own valid range on variable x.

2.2 Characteristics of the proposed equation

Figure 2 shows example curves illustrating the influences of the parameters a_1, a_2 and a_3 on the S-shape relationship. It can be shown that the proposed function has the following features.

(*a*) The asymptotic line for the proposed function is $y = b$ and the entire curve remains at one side of the asymptotic line, that is

$$3. \quad y \xrightarrow{x \to \infty} b$$

As seen in Equation 1, the function is rigidly translated along the y axis by the magnitude of b. Thus parameter b can be measured from the figure according to the translation of the S-shape relationship along the y axis.

(*b*) The value of $(y - b)$ varies linearly with the value of parameter a_1. This is clearly shown in Equation 1. Therefore, parameter a_1 is determined by the amplitude of the S-shape curve.

(*c*) The limit value for $(y - b)$, as x approaches zero, is as follows

$$4. \quad (y-b) \xrightarrow{x \to 0} \begin{cases} a_1 & \text{for } a_3 > 1 \\ a_1 + a_1 a_2 & \text{for } a_3 = 1 \\ \infty & \text{for } a_3 < 1 \end{cases}$$

The function has a singular point at $x = 0$ for $a_3 < 1$. The value of a_1 can be determined from Equation 4 for $a_3 > 1$. For $a_3 = 1$, an equation for parameters a_1 and a_2 is found, that is $a_1 + a_1 a_2 = (y - b)(x = 0)$.

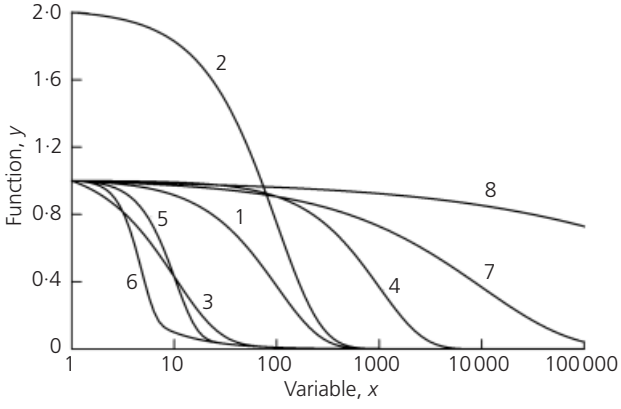

Figure 2. Influence of function parameters

(*d*) The value of the first part of the proposed equation monotonically approaches zero as x increases. The rate of the decrease for the absolute value of the first part is determined by parameters a_2 and a_3.

The values for function parameters presented in Figure 2 are listed in Table 1. A positive sign of the equation is assumed. $b = 0$ is assigned because the physical meaning of the parameter is clear.

Using curve 1 as a base for comparison, it is seen that an increase in the value of a_1 for curve 2 results in the amplification of the value of function y. For curve 3 the value for a_2 is increased ten times, and for curve 4 the value for a_2 is decreased ten times. It is seen that the main effect of a_2 is to shift the S-curve along the x axis. Four curves (curves 5–8) are presented to illustrate the effect of a_3, two of the curves with $a_3 > 1$, and the other two with $a_3 < 1$. It is clearly shown that the higher the value in a_3, the sharper the drop in y.

Parameter b can be measured directly from the S-shape curve. Parameter a_1, for $a_3 > 1$, can also be determined directly from the limit value of y as x approaches zero. For $a_3 = 1$, an equation for a_1 and a_2 can be obtained from the limit value of y as x approaches zero, which is given in Equation 4. Generally speaking, parameters a_1, a_2 and a_3 can be determined by fitting the theoretical curve with the known data because every parameter controls a distinct feature of the S-shape relationship.

3. The application

In this section, the proposed mathematical function is employed to make simulations of seven types of S-shape relationship observed in engineering and physics, and the capacity of the proposed function is evaluated according to its performance. All the experimental data are obtained from previous publications and they are marked by solid dots in Figure 1 and Figures 3–6.

3.1 Soil strength and the clay fraction

Two intrinsic strengths of soils, the critical state strength φ_{cs} and the residual strength φ_r are observed to be dependent on the clay fraction of the soil and there exists an S-shape relationship between the soil strengths and clay fraction (e.g. Lupini *et al.*, 1981;

Curve	a_1	a_2	a_3	b
1	1	0·01	1	0
2	2	0·01	1	0
3	1	0·1	1	0
4	1	0·001	1	0
5	1	0·01	2	0
6	1	0·01	3	0
7	1	0·01	0·5	0
8	1	0·01	0·3	0

Table 1. Values of function parameters

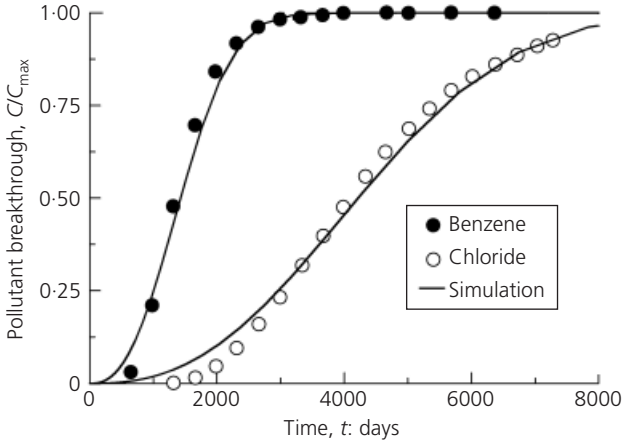

Figure 3. Breakthrough curves of chloride and benzene for sand–bentonite line (data after Van Ree *et al.*, 1992)

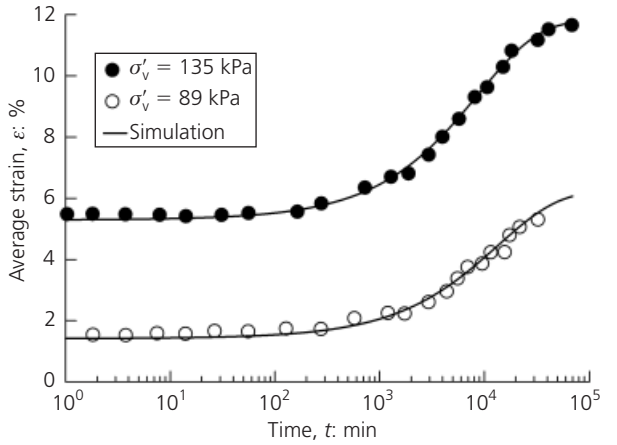

Figure 4. Creep behaviour of Drammen clay (data after Berre and Iversen (1972))

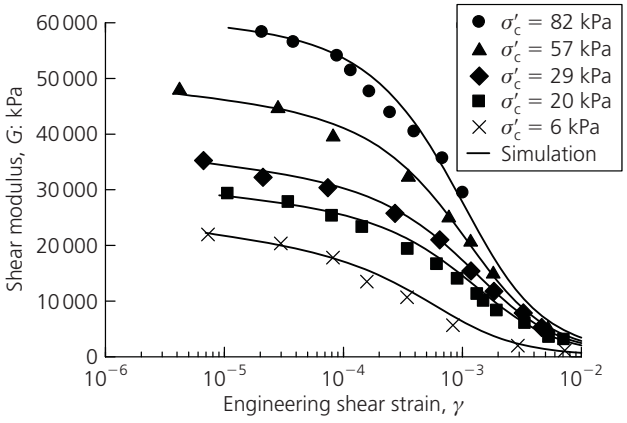

Figure 5. Variation of shear modulus with shear strain (data after Iwasaki *et al.* (1978))

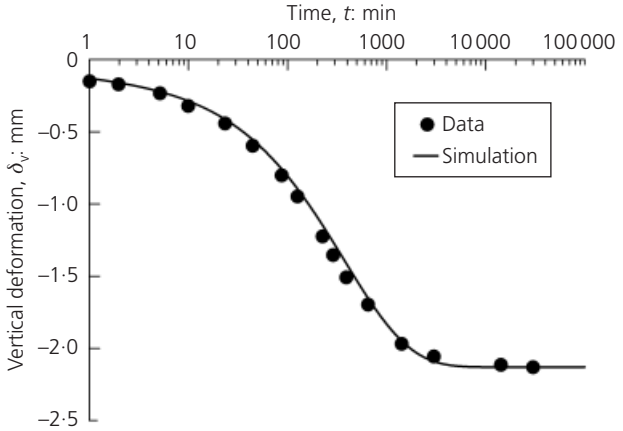

Figure 6. Vertical displacement with time for diatomaceous fill in an oedometer test (data after Day (1997))

Skempton, 1985). The experimental data from Lupini *et al.* (1981) on the variation of the two intrinsic strengths with clay fraction are quoted here for simulation (Figure 1(a)). The theoretical expressions for the soil strengths found are given below. ω_c is input as a percentage. The critical state friction angle

$$\phi_{cs} = \frac{12}{\omega_c}\left[1 + (\omega_c - 1)e^{-2\times10^{-5}\omega_c^{3\cdot2}}\right] + 20$$

5. $(0 \leqslant \omega_c \leqslant 100)$

The residual friction angle

$$\phi_r = \frac{26}{\omega_c}\left[1 + (\omega_c - 1)e^{-8\times10^{-6}\omega_c^{3\cdot3}}\right] + 5\cdot4$$

6. $(0 \leqslant \omega_c \leqslant 100)$

The theoretical curves generated by the above two equations are also shown in Figure 1(a) by solid lines.

3.2 Compression behaviour of soils

For the compression behaviour of soil under first loading, there exists an S-shape relationship between the voids ratio and the compressive effective stress if the soil is compressed from a very low stress level to the very high stress level, such as from 1 kPa to 10 000 kPa (e.g. Pestana and Whittle, 1995; Nagaraj *et al.*, 1990; Horpibulsuk *et al.* (2007)). The experimental data from Pestana and Whittle (1995) are quoted here for simulation (Figure 1(b)). The voids ratio is denoted by e, and the vertical effective stress is denoted by σ'_v. The theoretical expressions found for the three one-dimensional compression tests are given as follows. For the test with initial voids ratio $e = 1\cdot03$

$$e = \frac{0\cdot86}{\sigma'_v}\left[1 + (\sigma'_v - 1)e^{-2\cdot5\times10^{-3}\sigma_v'^{0\cdot64}}\right] + 0\cdot18$$

7. $(20\ \text{kPa} \leqslant \sigma'_v \leqslant 100\,000\ \text{kPa})$

For the test with initial voids ratio $e = 0\cdot906$

$$e = \frac{0\cdot74}{\sigma'_v}\left[1 + (\sigma'_v - 1)e^{-2\times10^{-3}\sigma_v'^{0\cdot65}}\right] + 0\cdot18$$

8. $(20\ \text{kPa} \leqslant \sigma'_v \leqslant 100\,000\ \text{kPa})$

For test with initial voids ratio $e = 0\cdot826$

$$e = \frac{0\cdot66}{\sigma'_v}\left[1 + (\sigma'_v - 1)e^{-1\cdot4\times10^{-3}\sigma_v'^{0\cdot68}}\right] + 0\cdot18$$

9. $(20\ \text{kPa} \leqslant \sigma'_v \leqslant 100\,000\ \text{kPa})$

A comparison between the theoretical curves and the experimental data is shown in Figure 1(b).

3.3 Pollutant breakthrough curves

It has been observed that the pollutant breakthrough curves for many materials are S-shaped (e.g. Rowe and Booker, 1985; Van Ree *et al.*, 1992). The experimental data from Van Ree *et al.* (1992) are shown in Figure 3. The normalised concentration parameter C/C_{max} increases from zero at $t = 0$ to 1 as time t increases. The unit for time is days. The tests include two materials, chloride and benzene. The following theoretical expressions are obtained for describing the breakthrough curves of the two pollutants. For benzene

$$\frac{C}{C_{max}} = -\frac{1}{t}\left[1 + (t - 1)e^{-9\times10^{-9}t^{2\cdot5}}\right] + 1$$

10. $(0 \leqslant t < \infty)$

For chloride

$$\frac{C}{C_{max}} = -\frac{1}{t}\left[1 + (t - 1)e^{-6\times10^{-10}t^{2\cdot5}}\right] + 1$$

11. $(0 \leqslant t < \infty)$

A comparison between the theoretical curves and the experimental data is shown in Figure 3. Even though the curves slightly divert from the experimental data at very short time period, the overall data are described well.

3.4 The S-shape relationship for the creep behaviour of soils

There are two types of creep behaviour, stable creep and unstable creep. For stable creep behaviour, the relationship between the strain ε and time t is usually S-shaped (e.g, Berre and Iversen, 1972; Yin and Graham, 1996). The data of one-dimensional compression tests on Drammen clay from Berre and Iversen (1972) are quoted here (Figure 4). Two tests with different vertical effective stresses σ'_v are considered. The theoretical expressions found for the creep behaviour of the two tests are given as follows. For $\sigma'_v = 135$ kPa

$$\varepsilon = -\frac{6{\cdot}5}{t}\left[1 + (t-1)\mathrm{e}^{-1{\cdot}1\times10^{-3}t^{0{\cdot}75}}\right] + 11{\cdot}8 \quad (0{\cdot}1 \text{ min} \leqslant t < \infty) \tag{12}$$

For $\sigma'_v = 89$ kPa

$$\varepsilon = -\frac{4{\cdot}8}{t}\left[1 + (t-1)\mathrm{e}^{-8\times10^{-4}t^{0{\cdot}75}}\right] + 6{\cdot}22 \quad (0{\cdot}1 \text{ min} \leqslant t < \infty) \tag{13}$$

In the equation, the unit for time is minutes and the strain calculated is a percentage. The theoretical curves are represented in Figure 4 by solid lines.

3.5 Shear moduli of geomaterials

It has been widely reported that for geomaterials there is an S-shape relationship between the shear modulus G and the shear strain γ (Hight *et al.*, 1992; Iwasaki *et al.*, 1978). The experimental data on the variation of shear modulus with shear strain from Iwasaki *et al.* (1978) are shown in Figure 5 by points. In the figure, there are six curves for Onahama sand under different confining pressures σ'_c. The units for both stress and modulus are kPa. The values of function parameters identified from the experimental data are listed in Table 2.

The theoretical curves generated by function parameters listed in Table 2 are shown in Figure 5 by solid lines. The parameters a_1, a_2 and a_3 are the best fitting for the range of strains considered.

Curve	a_1	a_2	a_3	b
$\sigma'_c = 82$ kPa	34·3	1550	0·99	0
$\sigma'_c = 57$ kPa	28·4	1300	0·98	0
$\sigma'_c = 29$ kPa	24·5	1000	0·97	0
$\sigma'_c = 20$ kPa	20·6	1000	0·97	0
$\sigma'_c = 10$ kPa	10·3	1400	0·95	0
$\sigma'_c = 5$ kPa	6·9	1800	0·95	0

Table 2. Values of function parameters

3.6 Consolidation and creep behaviour of soils

In an oedometer test, the vertical displacement, denoted by δ_v, is made up of two parts, namely the part contributed by the increment in the effective stresses and the part contributed by creep effect. The former is usually defined as primary consolidation, and the latter is defined as secondary consolidation. The total settlement plotted against time for a soil specimen in an oedometer test is usually S-shaped (Day, 1997; Ladd *et al.*, 1977). The experimental data from an oedometer test on diatomaceous fill reported by Day (1997) are simulated (Figure 6). The total vertical stress is maintained at 50 kPa for the test. The theoretical expression found is

$$\delta_v = \frac{2}{t}\left[1 + (t-1)\mathrm{e}^{-0{\cdot}02t^{0{\cdot}66}}\right] - 2{\cdot}13 \quad (0{\cdot}1 \text{ min} \leqslant t < \infty) \tag{14}$$

The vertical settlement δ_v is defined as negative and its unit is millimetres. The unit for time t is minutes. A comparison between the theoretical curves and the experimental data is shown in Figure 6.

3.7 Consolidation deflection of circular rafts

The consolidation deflection of a raft on a deep layer of soil plotted against time is an S-shape relationship (Booker and Small, 1984; Gibson *et al.*, 1970). The time deflection at the centre of a circular raft with various flexibility reported by Booker and Small (1984) is shown in Figure 1(c). In the figure, δ_c is the deflection at the centre of a circular raft normalised by the uniform loading acting on the raft; T' is a time factor and is defined as $T' = ct/a^2 \times 1000$, where c is the coefficient of one-dimensional consolidation, t is time and its unit is minutes and a is the radius of the circular raft.

The theoretical expressions found are given as follows

For $K = 0$

$$\delta_c = -\frac{0{\cdot}9}{T'}\left[1 + (T'-1)\mathrm{e}^{-0{\cdot}05\sqrt{T'}}\right] + 1{\cdot}93 \quad (1 \leqslant T' < \infty) \tag{15}$$

For $K = 1$

$$\delta_c = -\frac{0{\cdot}7}{T'}\left[1 + (T'-1)\mathrm{e}^{-0{\cdot}042\sqrt{T'}}\right] + 1{\cdot}62 \quad (1 \leqslant T' < \infty) \tag{16}$$

For $K = \infty$

$$\delta_c = -\frac{0{\cdot}62}{T'}\left[1 + (T' - 1)e^{-0{\cdot}042\sqrt{T'}}\right] + 1{\cdot}45 \quad (1 \leqslant T' < \infty) \qquad 17.$$

The curves generated by the above three expressions are also shown in Figure 1(c) by solid lines.

4. Discussion

Seven types of S-shape relationship encountered in geotechnical engineering practice are considered. Five of them describe material properties which are independent of the material size. They are

(*a*) peak shear strength of clayey soil
(*b*) compression behaviour of soil
(*c*) breakthrough curves for pollutants
(*d*) creep behaviour of soils
(*e*) shear moduli of geomaterials.

The other two describe the response of a system and the quantitative features of the responses are associated with a particular system only. They are

(*a*) consolidation and creep behaviour of soil in an oedometer test
(*b*) deflection of a circular raft with time.

Comparing the simulations and the experimental data, it is seen that all those S-shape relationships in both normal x and y scale and the semi-logarithmic x and y scale have been successfully represented by the proposed new mathematical function.

The following features are observed in simulating S-shape relationships of materials.

(*a*) Situations with both $a_3 \geqslant 1$ and $0 < a_3 < 1$ are encountered in engineering practice.
(*b*) For situations with $a_3 \geqslant 1$, the simulation by way of the proposed function is usually valid for the total valid range for x defined by the practical problem. However, for a situation with $0 < a_3 < 1$, the simulation by way of the proposed function is usually valid only for the range simulated. To illustrate the point, the valid range for Equations 15 through 17 is $1 \leqslant T' < \infty$, which is the range simulated. However, the valid range of this practical problem is $0 \leqslant T' < \infty$. It is also observed that data obtained by extrapolation for the former case are more reliable than for the latter case.
(*c*) For situations with $a_3 \geqslant 1$ two of the parameters are determined by fitting. The determination of the function parameters is found to be simple and direct according to the features that each parameter control. It appears that a unique set of parameters may be determined by fitting. For situations with $0 < a_3 < 1$ all the three parameters are determined by fitting, and the technique of trial and error may be required. Compared with the former situation, the values of function parameters are more sensitive to the range of variable x for simulation.

5. Conclusion

In engineering and physics, it has often been observed that some material characteristics and system responses exhibit an S-shape relationship. A new mathematical function is proposed for describing this relationship in both normal x and y scale and the semi-logarithmic x and y scale. The proposed function has been used to simulate the S-shape relationship of seven types of engineering phenomena, and it has been demonstrated that the proposed mathematical function describes all the events satisfactorily and can be used for characterising properties of materials or systems and thus is valuable for further numerical analysis.

Acknowledgements

The authors would like to express their thanks to Professors H. G. Poulos, J. P. Carter and B. Indraratna for the useful discussions and assistance in preparing this paper. The authors would also like to acknowledge their appreciation of the financial support from the Suranaree University of Technology.

REFERENCES

Berre T and Iversen K (1972) Oedometer tests with different specimen heights on a clay exhibiting large secondary compression. *Géotechnique* **22(1)**: 53–70.

Booker JR and Small JC (1984) The time–deflection behaviour of a circular raft of finite flexibility on a deep clay layer. *International Journal for Numerical Analytical Methods in Geomechanics* **8(4)**: 343–357.

Burland JB (1990) On the compressibility and shear strength of natural soils. *Géotechnique* **40(3)**: 329–378.

Butterfield R and Baligh F (1996) A new evaluation of loading cycles in an oedometer. *Géotechnique* **46(3)**: 547–553.

Day RW (1997) Discussion on 'engineering properties of diatomaceous fill' closure by Day. *Journal of Geotechnical and Geoenvironmental Engineering, ASCE* **123(6)**: 589–592.

Gibson RE, Schiffman RL and Pu SL (1970) Plane strain and axially symmetrical consolidation of a clay on a smooth impervious base. *Quarterly Journal of Mechanics and Applied Mathematics* **23(4)**: 505–519.

Hight DW, Bond AJ and Legge JD (1992) Characterisation of the Bothkennar clay: an overview. *Géotechnique* 42**(2)**: 303–347.

Horpibulsuk S, Liu MD, Liyanapathirana DS and Suebsuk J (2010) Behavior of cemented clay simulated via the theoretical framework of the structured Cam Clay model. *Computers and Geotechnics* **37(1–2)**: 1–9.

Horpibulsuk S, Shibuya S, Frenkajorn K and Katkan W (2007) Assessment of engineering properties of Bangkok clay. *Canadian Geotechnical Journal* **44(2)**: 173–187.

Khalili N, Habte MA and Valliappan S (2005) A bounding surface

plasticity model for cyclic loading of granular soils. *International Journal for Numerical Methods in Engineering* **63(14)**: 1939–1960.

Iwasaki T, Tatsuoka F and Takagi Y (1978) Shear moduli of sands under cyclic torsional shear tests. *Soils and Foundations* **18(1)**: 39–56.

Ladd CC, Foott R, Ishihara K, Schlosser F and Poulos HG (1977) Stress–deformation and strength characteristics. *Proceedings of the 9th International Conference on Soil Mechanics and Foundation Engineering, Tokyo, Japan*, vol. 2, pp. 421–494.

Liu MD and Carter JP (2003) The volumetric deformation of natural clays. *International Journal of Geomechanics, ASCE* **3(3/4)**: 236–252.

Lupini JF, Skinner AE and Vaughan PR (1981) The drained residual strength of cohesive soils. *Géotechnique* **31(2)**: 181–213.

Nagaraj TS, Srinivasa Murthy BR, Vatsala A and Joshi RC (1990) Analysis of compressibility of sensitive clays. *Journal of Geotechnical Engineering, ASCE* **116(GT1)**: 105–118.

Pestana JM and Whittle AJ (1995) Compression model for cohesionless soils. *Géotechnique* **45(4)**: 621–631.

Rowe RK and Booker JR (1985) 1-D pollutant migration in soils of finite depth. *Journal of Geotechnical Engineering, ASCE* **111(4)**: 479–499.

Skempton AW (1985) Residual strength of clays in landslides, folded strata and the laboratory. *Géotechnique* **35(1)**: 1–18.

Suebsuk J, Horpibulsuk S and Liu MD (2010) Modified structured Cam Clay: A constitutive model for destructured, naturally structured and artificially structured clays. *Computers and Geotechnics* **37(7–8)**: 956–968.

Suebsuk J, Horpibulsuk S and Liu MD (2011) A critical state model for overconsolidated structural clays. *Computers and Geotechnics* **38(5)**: 648–658.

Terzaghi K and Peck RB (1948) *Soil Mechanics in Engineering Practice*. Wiley, New York, NY, USA.

Van Ree CCDF, Weststrate FA, Meskers CG and Bremmer CN (1992) Design aspects and permeability testing of natural clay and sand-bentonite liners. *Géotechnique* **42(1)**: 49–56.

Yin JH and Graham J (1996) Elastic visco-plastic modelling of one-dimensional consolidation. *Géotechnique* **46(3)**: 515–527.